Immortalization of different breast epithelial cell types results in distinct mitochondrial mutagenesis.

Sujin Kwon[1], Susan S. Kim[3], Howard E. Nebeck[1], Eun Hyun Ahn[1,2,*]

[1]Department of Pathology, University of Washington, Seattle, WA 98195, USA
[2] Institute of Stem Cell and Regenerative Medicine, University of Washington, Seattle, WA 98109, USA
[3] Department of Biochemistry, University of Washington, Seattle, WA 98195, USA

*Correspondence to: ahneun@uw.edu

Abstract

Different phenotypes of normal cells might influence genetic profiles, epigenetic profiles, and tumorigenicities of their transformed derivatives. In this study, we investigated whether the whole mitochondrial genome of immortalized cells can be attributed to different phenotypes (stem versus non-stem) of their normal epithelial cell originators. To accurately determine mutations, we employed Duplex Sequencing, which exhibits the lowest error rates among currently available DNA sequencing methods. Our results indicate that the vast majority of observed mutations of the whole mitochondrial DNA occur at low-frequency. The most prevalent mutation types are C →T/G→A and A→G/T→C transitions. Frequencies and spectra of homoplasmic (high-frequency) point mutations are virtually identical between stem cell-derived immortalized (SV1) cells and non-stem cell-derived immortalized (SV22) cells, verifying that both cell types were derived from the same woman. However, frequencies of rare point mutations are significantly lower in SV1 cells (5.79×10^{-5}) than in SV22 cells (1.16×10^{-4}). Additionally, the predicted pathogenicity for rare mutations in the mitochondrial tRNA genes is significantly lower (by 2.5-fold) in SV1 cells than in SV22 cells. Our findings suggest that the immortalization of normal cells with stem cell features leads to decreased mitochondrial mutagenesis, particularly in noncoding RNA regions. The mutation spectra and mutations specific to stem cell-derived immortalized cells (versus non-stem cell derived) have implications in characterizing heterogeneity of tumors and understanding the role of mitochondrial mutations in immortalization and transformation of human cells.

Key words: Mitochondrial DNA, rare mutation, stem cells, breast cancer, tRNA, Duplex Sequencing, next generation sequencing

Introduction

Diverse phenotypes of tumors are often attributed to genetic and epigenetic alterations. However, evidence exists that distinct phenotypes of the normal cell originators for tumor derivatives also account for tumor heterogeneities [Bocker et al 2002, Dontu et al 2003, Welm et al 2003, Ince et al 2007, Keller et al 2012, Santagata et al 2014, Bu et al 2019]. For example, Ince et al (2007) reported that breast tumorigenic cells that were transformed respectively from two different normal epithelial cell types (BPECs; HMECs) exhibited marked differences in histopathology, tumorigenicity, and metastatic abilities. Transformed BPECs caused lung metastases, whereas transformed HMECs were nonmetastatic [Ince et al 2007]. Transformed BPECs were up to 104-fold more tumorigenic than transformed HMECs.

To study consequences of normal cell origins on genetic changes in their immortalized derivatives, we investigated two different immortalized (pre-neoplastic) breast epithelial cell types, which were derived from normal human breast epithelial cells (HBECs) with different phenotypes (Types I and II). Type I and Type II normal HBECs were isolated from breast tissue of the same woman; however, they exhibited different phenotypes. Type I HBECs display stem cell characteristics and have been characterized by: the expression of a stem cell marker octamer-binding transcription factor 4 (Oct-4) [Tai et al 2005] and estrogen receptor (ER)-α [Kang et al 1997], and luminal epithelial markers [Kao et al 1995, Kao et al 1997]; a deficiency in gap-junction

associated intercellular communication (GJIC) [Kao et al 1995, Chang et al 2001]; the ability to display anchorage-independent growth [Chang et al 2001]; the ability to differentiate into Type II (normal differentiated) HBECs [Kao et al 1995, Chang et al 2001]; reduced expression of maspin [Ahn et al 2006]; and the ability to form budding/ductal organoids on Matrigel in conjunction with Type II HBECs [Chang et al 2001]. In contrast, Type II HBECs exhibit opposite phenotypes in the described features above (i.e., do not express stem cell markers; do not express ER-α; express basal epithelial markers; express GJIC proteins; higher expression of maspin).

Both Type I (stem cell features) and Type II (without stem cell features) HBECs were transformed with Simian virus 40 large T-antigen (SV40-T) into immortal/non-tumorigenic (pre-neoplastic) cells, M13SV1 and M13SV22, respectively. SV40-T is widely used to immortalize and transform mammalian cells [Ahuja et al 2005, Pipas et al 2009]. Type II HBECs are less susceptible to SV40-T transformation than are Type I HBECs, and rarely become immortal following transfection with this virus [Kao et al 1995, Kang et al 1997, Sun et al 1999, Chang et al 2001]. This suggests that Type I HBECs and Type I HBEC-derived immortalized cells appear to be the major target cells for breast carcinogenesis and transformation.

In the present study, we examined whether the whole mitochondrial genome of these different immortalized human breast epithelial cell types is influenced by phenotypes of their originator normal HBECs (Type I and Type II). To accurately investigate low-frequency (heteroplasmic) rare and subclonal mutations as well as high-frequency (homoplasmic) mutations, we applied Duplex Sequencing (DS), which detects mutations with unprecedented accuracy [Schmitt et al 2012, Kenney et al 2014, Schmitt et al 2015, Ahn and Lee 2019]. Unlike conventional sequencing technologies that sequence only a single strand of DNA, DS sequences both strands of DNA and scores mutations only if they are present in both strands of the same DNA molecule as complementary substitutions. This significantly lowers background error rates (eg., Next generation sequencing error rates 10^{-2} to 10^{-3}; DS error rates < 5×10^{-8}) [Schmitt et al 2012, Lou et al 2013, Fox et al 2014, Kennedy et al 2014, Ahn and Lee 2019].

Results

In this study, stem cell-derived immortalized human breast epithelial cells (HBECs) will be referred to as SV1 and non-stem cell-derived immortalized HBECs will be referred to as SV22 cells. Both SV1 and SV22 cells were cultured under the same conditions, DNA was extracted, and DNA libraries were prepared for Duplex Sequencing (DS) as we have described previously [Ahn et al 2015]. The average number of nucleotides at each genome position (depth) was calculated as the total number of duplex consensus sequence (DCS) nucleotides sequenced divided by the mtDNA size of 16569 bases. The DCS depths were 1666 for SV22 (all Figures and Tables) and 1060 (all Tables and Figures except Fig S5) for SV1 and 2738 (Fig S5) for SV1. These are estimated to be equivalent to single-strand tag-based sequencing depths of approximately 7900 to 9800 and 5000 to 6200, respectively [Ahn and Lee 2019].

We have defined mtDNA mutations (variants) found in SV1 and SV22 cells as homoplasmic (90-100%), subclonal (0-10%) and rare (0-1%) based on the mutation occurrence (%) at each genome position. Maternally inherited mitochondrial mutations arising during early embryonic development are more likely to be homoplasmic [Taylor et al 2005, Chan et al 2006]. In the present study, we focused on rare and subclonal variants, as they presumably represent *de novo* somatic variants. Rare or subclonal mutations are not accurately determined by conventional next generation sequencing methods due to their high background error frequencies (10^{-2} to 10^{-3}) [Lou et al 2013, Fox et al 2014, Salk et al 2018]. These rare and subclonal mutations, however, are accurately detectable by Duplex Sequencing [Schmitt et al 2012, Kenney et al 2014, Schmitt et al 2015, Ahn and Lee 2019].

Both SV1 and SV22 cells exhibit identical homoplasmic mutations, verifying that both cell types were derived from the same individual. Thirty-five identical homoplasmic unique mutations were found between the two cell types (**Fig S1**). Frequencies, types (%), and context fractions (%) of homoplasmic mutations were almost identical (**Fig S1**) in both cell types. T>C/A>G and C>T/G>A transitions are the only mutation types observed with T>C/A>G being more dominant than C>T/G>A (**Fig S1**). As homoplasmic

mitochondrial mutations are presumably maternally inherited mutations, our results of identical homoplasmic mutations in both cell types verify that they were derived from the same woman.

SV1 cells show significantly lower frequencies of rare mutations and subclonal mutations than do SV22 cells. We determined frequencies of rare and subclonal mutations in SV1 (stem) and SV22 (non-stem) cells by Duplex Sequencing. The overall frequencies of both rare (**Fig 1A**) and subclonal (**Fig S2A**) mutations are significantly lower in SV1 cells (by 2-fold) than in SV22 cells. In addition, we determined frequencies of each point mutation type, of insertions, and of deletions. C>T/G>A and T>C/A>G transitions are the most dominant types for both SV1 and SV22 cell types (**Figs 1B-D**, **Figs S2B-D**). Frequencies of each type of rare and subclonal mutations are also significantly lower in SV1 cells than in SV22 cells (**Figs 1B, S2B**).

The strand bias of rare and subclonal mutations are observed in both cell types.
The two strands of mtDNA are designated as heavy (H) and light (L) strands [Strachan and Read 1999]. Our Duplex Sequencing data are referenced to the L-strand. In the L-strand of both SV1 and SV22 cells, C>T are significantly more prevalent than G>A; T>C are significantly more prevalent than A>G; A>C are significantly more prevalent than T>G; C>A are significantly more prevalent than G>T (**Figs 1C-D**, **S2C-D**). These significant asymmetric distributions within the complementary mutation type reflect a strand orientation bias in both cell types.

C>T/G>A transitions are the most prevalent mutation types followed by T>C/A>G in both SV1 and SV22 cells. The fraction (%) of rare and subclonal mutation types in SV1 (stem) and SV22 (non-stem) cells were calculated (**Figs 2A**, **S3A**). In both SV1 and SV22 cells, the most prevalent rare and subclonal mutation types are C>T/G>A and T>C/A>G (**Figs 2A**, **S3A**). The percentages of C>T/G>A and T>C/A>G rare mutations are similar between both cell types. In contrast, the fractions of the four rare mutation types in SV1 and SV22 cells are different by about 1.5-fold with higher fractions of C>A/G>T mutation types in SV1 cells and higher fractions C>G/G>C, T>C/A>G, and T>G/A>C mutation types in SV22 cells (**Fig 2A**).

To investigate influences of neighboring bases on types of rare and subclonal mutations, the bases immediately 5' and 3' to each mutated base were identified (i.e. the mutation occurs at the second position of each such trinucleotide). This allows classification of observed substitutions into 96 categories (4 bases X 6 substitutions x 4 bases). Numbers and fractions (%) of these mutation trinucleotides in each of the categories compose the "mutation context spectra" (MCS) of the cells. For both rare and subclonal mutations, T>G transversions in context G<u>T</u>A were significantly lower (p=0.02) in SV1 than in SV22 cells (**Figs 2B-C**, **S3B-C**).

The decreased mitochondrial mutagenesis of SV1 cells occurs mainly in the noncoding RNA region (rRNA and tRNA) of the mitochondrial genome. The human mitochondrial genome consists of three regions: protein coding (13 genes), non-coding (nc) RNA (2 rRNA and 22 tRNA genes), and control/overlapped regions. We examined which region of the three regions is more vulnerable to mitochondrial mutagenesis (**Fig 3A, Table S1**) in SV1 and SV22 cells.

Of the three categorized regions, the ncRNA regions exhibit the most significant differences in the number of rare mutations between SV1 and SV22 cells. The number of rare unique mutations in the ncRNA regions is significantly lower in SV1 cells than in SV22 cells (**Fig 3A, Table S1**; $p = 2.6\text{x}10^{-15}$). However, the sizes of the three regions are different, contributing to a bias in the number of observed unique mutations. In particular, the number of bases of the protein coding regions (11341) is greater than that of the ncRNA (4020) and the control/overlapped regions (approximately 1772) [Govatati et al 2013]. Thus, to compare mutation prevalence per the same genome size between protein-coding regions and ncRNA regions, we estimated the number of rare unique mutations per 1000 bases and found an even more significantly higher number of rare unique mutations in ncRNA regions than in the protein coding regions. This indicates that the ncRNA

regions are more susceptible to mitochondrial mutagenesis than the protein-coding regions. Within the ncRNA region itself, there is a significantly lower number of rare unique mutations in SV1 cells than in SV22 cells (**Fig 3B**, **Table S2**; $p = 1x10^{-4}$). Genome position and clonality (%) for each of rare mutations observed in SV1 and SV22 cells are presented in **Figure 4A**,**B**. The average and median clonalities (%) of rare mutations are still about 1.7-fold significantly lower in SV1 cells (0.17% $\pm$ 0.006) than in SV22 cells (0.29% $\pm$ 0.007), even after excluding variants that were mutated only once (singlet mutations) (**Fig 4C,D**).

Proportions (%) of nonsynonymous mutations in mitochondrial protein coding regions and their predicted pathogenicity scores of subclonal mutations are similar between SV1 and SV22 cells. We compared the proportion (%) of nonsynonymous mutations (causing changes in amino acids) of mitochondrial protein coding regions between SV1 and SV22 cells. Overall, no significant differences in rare or subclonal mutations were observed in the mitochondrial protein coding region between the two cell types (**Table S3**).

Predicted pathogenicity scores of missense mutations of mitochondrial protein coding regions are similar between SV1 and SV22 cells. Predicted pathogenicity scores of the subclonal missense mutations were evaluated using MutPred program version 2.0 (http://mutpred.mutdb.org) [Pejaver et al 2017]. MutPred provides a general *g* score for each missense mutation, where a higher *g* score indicates a higher chance that an amino acid substitution is deleterious. The *g* scores were obtained for each of subclonal missense mutations present only in SV22 cells, and for those present only in SV1 cells, but not for those present in both cell types. A total of 153 subclonal missense mutations and 9 nonsense mutations were found only in SV22 cells. A total of 142 subclonal missense mutations and 11 nonsense mutations were found only in SV1 cells. The sum of *g* scores for each of the 13 mtDNA protein-coding genes was calculated for both cell types and no significant difference was found in the average of *g* score sums between SV1 and SV22 cells (**Fig S4**).

Predicted pathogenicity scores of rare mutations of mitochondrial tRNA genes tend to be lower in SV1 cells than in SV22 cells. Variants in mt-tRNA genes are a common cause of mitochondrial disease [Sonney et al 2017]. Thus, we evaluated whether rare and subclonal mutations in tRNA genes of the mtDNA genome would alter protein function and increase the predicted pathogenicity by using the mitochondrial tRNA informatics predictor (MitoTIP) program of MITOMAP [Sonney et al 2017]. MitoTIP provides a raw score, which is derived from three sub-scores: variant history and conservation score, position score, and secondary structure score. A higher score represents a higher probability of pathogenicity.

The pathogenicity raw scores were obtained for both rare and subclonal mutations in each of 22 mt-tRNA genes. We compared pathogenicity scores of mt-tRNA gene mutations found specifically in SV1 cells *vs* in SV22 cells. Eighty-three rare mutations were present in SV22 cells only; while 31 rare mutations were found in SV1 cells only. The exact same mutations specific to each cell type (SV1 *vs* SV22) were observed in the subclonal range. The average pathogenicity score of mt-tRNA mutations tends to be lower in SV1 cells than in SV22 cells (**Fig 5**; p = 0.082). In addition, we found four known/confirmed pathogenic tRNA variants (m.5650 G>A, m.5521 G>A, m.5690 A>G, m. 1630 A>G) among the 83 variants in SV22 cells, whereas confirmed pathogenic tRNA variants were not found in SV1 cells.

Duplex Sequencing identifies many rare or subclonal mutations that are specific to SV1 and to SV22 cells. To compare positions of mutations between SV1 and SV22 cells, only genome positions that had DCS read counts at least 100 or higher in both cell types were considered. Mutations occurring at the same genome positions were scored only once and referred as unique mutations. We have identified rare and subclonal unique mutations that are present only in SV22 cells versus SV1 cells or in both cell types.

A total of 527 rare and 528 subclonal mutations were found in SV1 cells only (but not in SV22 cells); 792 rare and 797 subclonal mutations were found in SV22 cells only (but not in SV1 cells) (**Table S4**). 447

rare mutations were found in both SV1 and SV22 cells, of which 88 mutations are more prevalent in SV22 than in SV1 and 9 mutations are more prevalent in SV1 than in SV22 (prevalence meaning by at least a 3-fold difference) (**Table S4**). Similarly, 459 subclonal mutations were found in both SV1 and SV22 cells, of which 92 mutations are more prevalent in SV22 than in SV1 and 11 mutations are more prevalent in SV1 than in SV22 by at least a 3-fold difference (**Table S4**).

A detailed list of subclonal unique mutations, in which variant reads are at least two or greater, is presented in **Table S5**. Mutations were considered singlets if they have a variant read of 1, and these were excluded in **Table S5**. A total of 122 non-singlet subclonal mutations were observed only in SV1 cells but not in SV22 cells, whereas 190 non-singlet subclonal mutations were observed only in SV22 cells but not in SV1 cells (**Table S5A, S5B**). Among the identified subclonal mutations present in both SV1 and SV22 cells, 92 subclonal mutations were more highly mutated in SV22 cells than in SV1 cells by at least 3-fold (**Table S5C**). In contrast, only 11 subclonal mutations were more highly mutated in SV1 cells than in SV22 cells by at least 3-fold (**Table S5D**).

Independent DNA library preparation experiments of Duplex Sequencing produce reproducible results. Two independent DNA library preparation experiments were performed for SV1 cells. Consistent results of frequencies (**Fig S5A**), types (%) (**Fig S5B**), and sequence context spectra (%) of rare mutations (**Fig S5C-D**) were obtained from the two independent experiments. This validates the reproducibility of our Duplex Sequencing data.

Discussion

Ince et al (2007) reported that transformation of different normal human breast epithelial cell types led to distinct neoplastic phenotypes. Such differences align with findings that the same oncogenes can have quite different phenotypic consequences depending on the cell origin [Vogelstein and Kinzler 2004, Gupta and Massague 2006]. Taken together, these suggest that the pre-existing differences in originator normal cell types significantly influence phenotypes of their transformed cells. Gordon et al (2014) demonstrated that immortalization of human fetal lung fibroblasts increased DNA methylation at gene promoters and caused large-scale changes in gene expression. While these studies [Ince et al 2007, Gordon et al 2014] have examined tumorigenicity, histopathology, and metastatic behavior of human breast transformed cells and DNA methylation and gene expression of human fibroblasts, no study has examined the subclonal mutations of the whole mitochondrial genome for immortalized derivatives of phenotypically different normal cells.

In the current study, using Duplex Sequencing, we systemically examined mutations of the whole mitochondrial genome for two types of immortalized HBECs (SV1 vs SV22), specifically, HBECs transformed from stem *vs* non-stem cells with SV40-T. Our data indicate that both rare and subclonal mutation frequencies are significantly lower in SV1 cells than in SV22 cells (**Figs 1, S2**). Previously, we compared rare mutations of the whole mitochondrial genome between paired normal HBECs (stem versus non-stem cells) from three independent women and we observed that normal stem cells from two women exhibited significantly lower frequencies of rare mutations than the matching non-stem cells [Ahn et al. 2015]. Our previous [Ahn et al 2015] and current findings suggest that the significant lower frequencies of rare and subclonal mutations of the whole mitochondria genome in stem cell-derived immortalized (SV1) cells can be attributed to mitochondrial mutations of their parental originator normal cell types. It supports the idea that distinct normal breast epithelial cell types lead to different mitochondrial mutagenesis in their immortalized/transformed cells.

Mechanisms for the lower frequencies of subclonal mutations in stem cell-derived immortalized breast cells (**Fig S2B**) than in non-stem cell-derived immortalized cells are unclear. A possible mechanism might be associated with lower levels of reactive oxygen species (ROS). The lower ROS levels in stem cells could lead to reduced mtDNA damage and accumulation of subclonal mutations [Saretzki et al 2008, Frosina 2010]. Stem cells might have more efficient systems of DNA repair and mitophagy for removing damaged mtDNA, therefore, lowering the number of mtDNA mutations generated [Frosina et al 2010, Guan et al 2013, Joshi and Kundu

[2013]. These lower ROS levels and reduced mtDNA mutations of normal stem cells could be continually passed down to their immortalized cells.

Our results indicate that rare mutations are more prevalent in the non-coding RNA (ncRNA) regions (mt rRNA 12s; mt rRNA 16s; mt tRNAs) than in the protein coding and control regions (**Fig 3**). Furthermore, the largest decrease in rare mutation burden in SV1 cells versus in SV22 cells is observed in the ncRNA region (**Fig 3**). In ncRNA regions, the pathogenicity of mt tRNA mutations can be predicted using the analysis tool MitoTIP. We demonstrated that predicted pathogenicity scores of rare mutations in mt-tRNA genes were significantly lower in SV1 cells than in SV22 cells (**Fig 5**). This indicates that the lower rare mutation burden of ncRNA genes in SV1 are accompanied with lower predicted pathogenicity.

Furthermore, we demonstrate that four known pathological mt-tRNA gene mutations, m.5650 G>A (mt-tRNA^{Ala}) [McFarland et al 2008], m.5521 G>A (mt-tRNA^{Trp}) [Porcelli et al 2010], m.5690 A>G (mt-tRNA^{Asn}) [Blakely et al 2013], and m.1630 A>G (mt-tRNA^{Val}) [Horvath et al 2009, Glatz et al 2011] were present in SV22 cells. However, no known pathogenic mutations were found in the mt-tRNA genes of SV1 cells. Pathogenicity of these four mt-tRNA mutations were confirmed by several studies [McFarland et al 2008, Porcelli et al 2010, Blakely et al 2013, Horvath et al 2009, Glatz et al 2011]. All of the four confirmed pathogenic mutations are related to causing myopathy, a common mitochondrial disease effectuated by impacting protein translation or affecting tRNA stability [McFarland et al 2008, Porcelli et al 2010, Blakely et al 2013, Horvath et al 2009, Glatz et al 2011]. Cytochrome c oxidase (COX)-deficiency was commonly reported with all four mutations [McFarland et al 2008, Porcelli et al 2010, Blakely et al 2013, Horvath et al 2009, Glatz et al 2011]. The m.5650 G>A mutation causes a phenotype of pure myopathy [McFarland et al 2008] and disrupts interaction between mitochondrial alanyl-tRNA sythetase and mt-tRNA^{Ala} aminoacyl acceptor stem. The m.5521 G>A mutation may impact protein translation [Porcelli et al 2010]. The m.5690 A>G mutation manifested clinical presentations of chronic progressive external ophthalmoplegia and ptosis [Blakely et al 2013]. The m.1630 A>G mutation impairs oxygen consumption, which affects the stability of mt-tRNA^{Val} and reduces the levels of subunits of the electron transport chain [Glatz et al 2011]. Horvath et al (2009) reported that the m.1630 A>G mutation may cause mitochondrial neurogastrointestinal encephalomyopathy such as gastrointestinal dysmotility and cachexia [Horvath et al 2009].

In human breast cancer, tRNA mutations can cause significant consequences due to their important roles in protein translation [Meng et al 2015]. Mt-tRNA point mutations are typically caused by the loss of mt-tRNA stability, which leads to defective mitochondrial translation and respiratory chain deficiency [Blakely et al 2013] through: aberrant processing of mRNA transcripts by RNases P and ZL, impaired post-transcriptional mt-tRNA modification such as specific base modifications, 3-end additions of -CCA sequence and mt-tRNA aminoacylation, as well as compromised interaction of mt-tRNA with both mtEF-Tu (mitochondrial elongation factor Tu) and the mitoribosome [Levinger et al 2004]. Our results suggest that stem cell-derived immortalized (SV1) cells might possess a more stable mitochondrial genome, exhibited by lower subclonal mutation burden and lower predicted pathogenicity than non-stem cell-derived immortalized (SV22) cells.

In summary, we examined whether different phenotypes of originator normal human breast epithelial cells (stem *vs* non-stem) can lead to different profiles of mitochondrial mutations for their immortalized derivatives. Our results indicate that the vast majority of mutations in the cells occur at rare mutation levels, which are not detectable by conventional DNA sequencing methods, but are accurately detectable by Duplex Sequencing. The most prevalent rare mutation types are C>T/G>A and A>G/T>C transitions. Immortalized stem cells (SV1) exhibit lower frequencies of rare mutations than immortalized non-stem cells (SV22). The reduced mitochondrial rare mutation burden of immortalized stem cells mainly occurs in ncRNA regions of the whole mtDNA, and these are accompanied by reduced predicted pathogenicity. Our findings suggest that phenotypes of originator parental normal cells significantly influence and direct mutational profiles of the whole mitochondrial genome in their immortalized derivatives. Our results have implications in investigating genetic changes of mitochondrial genomes acquired during cellular immortalization and in characterizing immortalized stem (*vs* non-stem) cells, which represent *in vitro* preneoplastic stages of breast carcinogenesis.

Methods

Development and culture of immortalized human breast epithelial cells. Immortalized cells (M13SV1, M13SV22) were derived from paired groups (stem *vs* non-stem) of normal human breast epithelial cells (HBECs) treated with SV40 large T-antigen (SV40-T). M13SV1 cells were derived from normal HBECs with

stem cell features (Type I); M13SV22 cells were derived from normal HBECs without stem cell features (Type II). These immortalized cells were provided by Dr. Chia-Cheng Chang at Michigan State University (MSU) in East Lansing, MI, USA. A Material Transfer Agreement was approved by both MSU and University of Washington (UW). Development and characterization of normal HBEC and *in vitro* transformed HBECs have been described previously [Kao et al 1995, Kang et al 1997, Kang et al 1998, Chang et al 2001, Park et al 2004, Tai et al 2005, Ahn et al 2006, Ahn et al 2009, Wang et al 2010 (a), Ahn et al 2015].The cells were cultured at the UW as described previously [Kao et al 1995, Kang et al 1998, Chang et al 2001, Ahn et al 2016].

DNA extraction, adapter synthesis, and DNA library preparation for Duplex Sequencing (DS). DNA extraction and purification, adapter synthesis, and DNA library preparation for DS were carried out as described previously [Ahn et al 2015]. In short, DNA was extracted using Invitrogen DNA extraction kit, and Duplex Tag-labeled adapters with a single-nucleotide A or T overhang were subjected to end-repair on 3'dT-tailing or 3'-dA-tailing respectively of the sheared DNA. The whole mitochondrial genome was captured using Agilent SureSelect^{XT} target enrichment (Agilent Technologies).

Data processing. DS data were processed as described previously [Schmitt et al 2012, Kennedy et al 2014, Ahn et al 2015, Pickrell et al 2015] with modifications. Previously, our in-house DS script processed and aligned two sequence read files of pair-end sequencing separately and independently before merging the two read files. For the current study, the script was modified to merge two sequence read files first then process and align the merged file. This modification improved accuracy and efficiency of data processing. Sequence reads were aligned to the revised Cambridge Reference sequence (rCRS) reference genome (NC_012920) using BWA and the genome analysis toolkit (GATK) software as described previously [Ahn et al 2015]. BWA "mem" was used in replacement of BWA "aln". During processing, all datasets' reads were filtered using a mapping quality score of 40. Pileup-based variant calling used the default base quality score of 13. The first four bases at 5' and 3' ends of each sequence reads were clipped to eliminate potential artifactual variants commonly present at the ends of each read.

Data analysis for positions, frequencies, types, and context spectra of mutations and annotation of genetic variants. Genome positions with a DCS sequence read depth of 100 or greater were included for the data analysis. In addition, for comparing the mutations of SV1 and SV22 cells, only genome positions that had a minimum DCS read of 100 in matching positions of both samples were considered. The total number of DCS variant reads were divided by total number of DCS sequenced reads to calculate mutation frequencies for each sample. The total number of unique mutations (i.e. mutants were scored only once at each position of the genome regardless of number of variant reads observed in that position) were used for all other analyses, which includes fractions (%) of mutation types, mutation context spectra (%), and comparison of mutation positions.

Genetic variant data from Duplex Sequencing were annotated using Annotate Variation (ANNOVAR) bioinformatical software version 2017Jun01 (annovar.openbioinformatics.org) [Wang et al. 2010 (b)]. Annotations were added for each sequenced position of the whole mitochondrial genome.

Pathogenicity of point mutations in mitochondrial protein coding regions. The MutPred program version2.0 (http://mutpred.mutdb.org) [Pejaver et al 2017] was used to obtain predicted pathogenicity score for missense mutations present either in SV1 or SV22 cells, but not in both cell types. The program classifies amino acid substitutions as pathogenic or benign while predicting their impact on protein properties. A pathogenicity score between 0 and 1 is given to each missense mutation based on its impact. Pathogenicity scores can be obtained by submitting a list of missense mutations with a mitochondrial gene reference sequence (NC_012920) to the MutPred program.

Pathogenicity of point mutations in mitochondrial tRNA regions. The predicted pathogenicity scores for mt-tRNA mutations were analyzed using MitoTIP (August 2017 version) available *via* MITOMAP (www.mitomap.org). MitoTIP analysis [Sonney et al 2017] involves calculating pathogenicity scores for each possible variant through a summation of variant history, conservation score, position score, and secondary structure score. Using publicly available databases, an algorithm that estimates the importance of a position across mtDNA was generated and used in scoring. Pathogenicity scores ranged from -5.9 to 21.8 and were assigned to each variant in mt-tRNAs by its position.

Statistical analysis. Differences in mtDNA mutation frequencies and in the fraction (%) of mutation types between the two groups were analyzed by performing the prop.test for '2-sample equality of proportions with continuity correction' using an R program (version 3.4.4). To compare the MitoTIP predicted pathogenicity scores between the two groups, the Mann-Whitney U-test (Wilcoxon Rank-Sum test) was applied using Sigma Plot (version 12.0) (Systat Software, San Jose, CA). Differences between the two groups were considered significant if the p-value was less than 0.05.

Supplementary materials are available on line.

Author contributions: EHA conceived and designed the experiment; EHA performed the experiments; SK, SSK, HEN, and EHA processed sequencing data and/or analyzed the data; EHA, HEN, SK, and SSK wrote the paper.

Funding: The research was supported by grants from the National Institute of Environmental Health Sciences (NIEHS) P30 ES007033 sponsored-University of Washington (UW) Center for Exposures, Diseases, Genomics and Environment (EDGE) pilot grant (to EH Ahn), UW Office of Research Royalty Research Fund (to EH Ahn), and National Cancer Institute (NCI) P30 CA015704-39 Fred Hutchinson Cancer Research Center-UW Cancer Consortium Support Grant (to EH Ahn), NCI R21 CA220111 (to EH Ahn), and NCI of the National Institutes of Health (NIH) under award numbers P01 AG001751 and R33 CA181771 (to LA Loeb). The content is solely the responsibility of the authors and does not necessarily represent the official views of the NIH.

Acknowledgements: We thank Drs. Chia-Cheng Chang, Brad L. Upham, and James E. Trosko for obtaining immortalized human breast epithelial cells and Seung Hyuk (Tony) Lee for editing the manuscript.

Conflicts of interest: The authors declare no conflict of interest.

Figure legends

Figure 1. Frequencies of rare mutations in the whole mtDNA of SV1 and SV22 cells. Overall rare mutation frequency (**A**) and frequencies of rare mutation types (**B-D**) for SV1 and SV22 cells were determined using Duplex Sequencing. Error bars represent the Wilson Score 95% confidence intervals. Significant differences in rare mutation frequencies between two groups are indicated (* $p < 0.05$, ** $p < 5 \times 10^{-4}$, and *** $p < 5 \times 10^{-10}$) by the 2-sample test for equality of proportions with continuity correction.

Figure 2. Types and sequence context spectra of rare unique mutations in the whole mtDNA of SV1 and SV22 cells. Fractions (%) of rare mutation types (**A**) and fractions (%) of rare mutation context spectra (**B,C**) were determined using Duplex Sequencing. Trinucleotide contexts (**B,C**) are the mutated base surrounded by all possibilities for its immediate 5' and 3' bases. To keep the graph concise, these point mutation trinucleotides are complemented as necessary to always depict the reference base as the pyrimidine of its pair. The fraction (%) of each specific trinucleotide out of all 96 possible trinucleotide contexts depicts the contribution of each genome sequence context to each point mutation type. Significant differences in fractions (%) of mutation context types between the two groups are indicated (* $p < 0.05$) by the 2-sample test for equality of proportions with continuity correction).

Figure 3. Number of rare unique mutations considered (individually and per 1000 bases) by genome positional category in the whole mtDNA of SV1 and SV22 cells. Number of rare unique mutations by positional category (**A**) and number of rare unique mutations per 1000 bases by positional category (**B**) were determined using ANNOVAR software tool. Significant differences in numbers of rare mutations between the two groups are indicated (* $p < 0.05$, ** $p < 5 \times 10^{-4}$, and *** $p < 5 \times 10^{-10}$) by the 2-sample test for equality of proportions with continuity correction.

Figure 4. Genomic positions and clonalities (%) of rare unique mutations in the whole mtDNA of SV1 and SV22 cells. Rare mutation clonalities (%) by genomic position including singlets (**A,B**) or excluding singlets (**C,D**) were determined using Duplex Sequencing. Singlets are defined as variants that are mutated only once in nucleotides sequenced at a specific genome position.

Figure 5. Predicted pathogenicity of rare unique mutations of mt-tRNAs in SV1 and SV22 cells. Predicted pathogenicity scores of rare variants in mt-tRNAs were obtained using MitoTIP and then were totaled for each region of tRNAs. Only the mutations present exclusively in each sample (mt-tRNA mutations present only in SV1 *vs* mt-tRNA mutations present only in SV22) were included. The sums of predicted pathogenicity scores from each mt-tRNA region were averaged for SV1 and SV22 cells. Error bars represent the standard error of the mean (SEM).

References

Ahn, E.H.; Chang, C.-C.; Schroeder, J.J. Evaluation of sphinganine and sphingosine as human breast cancer chemotherapeutic and chemopreventive agents. *Exp. Biol. Med. (Maywood)* **2006**, *231*, 1664–1672.

Ahn, E.H.; Chang, C.-C.; Talmage, D.A. Loss of anti-proliferative effect of all-trans retinoic acid in advanced stage of breast carcinogenesis. *Anticancer Res.* **2009**, *29*, 2899–2904.

Ahn, E.H.; Hirohata, K.; Kohrn, B.F.; Fox, E.J.; Chang, C.-C.; Loeb, L.A. Detection of Ultra-Rare Mitochondrial Mutations in Breast Stem Cells by Duplex Sequencing. *PLoS ONE* **2015**, *10*, e0136216.

Ahn, E.H.; Lee, S.H. Detection of Low-Frequency Mutations and Identification of Heat-Induced Artifactual Mutations Using Duplex Sequencing. *Int J Mol Sci* **2019**, *20*.

Ahn, E.H.; Lee, S.H.; Kim, J.Y.; Chang, C.-C.; Loeb, L.A. Decreased Mitochondrial Mutagenesis during Transformation of Human Breast Stem Cells into Tumorigenic Cells. *Cancer Res.* **2016**, *76*, 4569–4578.

Ahuja, D.; Sáenz-Robles, M.T.; Pipas, J.M. SV40 large T antigen targets multiple cellular pathways to elicit cellular transformation. *Oncogene* **2005**, *24*, 7729–7745.

Blakely, E.L.; Yarham, J.W.; Alston, C.L.; Craig, K.; Poulton, J.; Brierley, C.; Park, S.-M.; Dean, A.; Xuereb, J.H.; Anderson, K.N.; et al. Pathogenic mitochondrial tRNA point mutations: nine novel mutations affirm their importance as a cause of mitochondrial disease. *Hum. Mutat.* **2013**, *34*, 1260–1268.

Böcker, W.; Moll, R.; Poremba, C.; Holland, R.; Van Diest, P.J.; Dervan, P.; Bürger, H.; Wai, D.; Ina Diallo, R.; Brandt, B.; et al. Common adult stem cells in the human breast give rise to glandular and myoepithelial cell lineages: a new cell biological concept. *Lab. Invest.* **2002**, *82*, 737–746.

Bu, W.; Liu, Z.; Jiang, W.; Nagi, C.; Huang, S.; Edwards, D.P.; Jo, E.; Mo, Q.; Creighton, C.J.; Hilsenbeck, S.G.; et al. Mammary Precancerous Stem and Non-Stem Cells Evolve into Cancers of Distinct Subtypes. *Cancer Res.* **2019**, *79*, 61–71.

Chan, D.C. Mitochondria: dynamic organelles in disease, aging, and development. *Cell* **2006**, *125*, 1241–1252.

Chang, C.C.; Sun, W.; Cruz, A.; Saitoh, M.; Tai, M.H.; Trosko, J.E. A human breast epithelial cell type with stem cell characteristics as target cells for carcinogenesis. *Radiat. Res.* **2001**, *155*, 201–207.

Dontu, G.; Al-Hajj, M.; Abdallah, W.M.; Clarke, M.F.; Wicha, M.S. Stem cells in normal breast development and breast cancer. *Cell Prolif.* **2003**, *36 Suppl 1*, 59–72.

Fox, E.J.; Reid-Bayliss, K.S.; Emond, M.J.; Loeb, L.A. Accuracy of Next Generation Sequencing Platforms. *Next Gener Seq Appl* **2014**, *1*.

Frosina, G. The bright and the dark sides of DNA repair in stem cells. *J. Biomed. Biotechnol.* **2010**, *2010*, 845396.

Glatz, C.; D'Aco, K.; Smith, S.; Sondheimer, N. Mutation in the mitochondrial tRNA(Val) causes mitochondrial encephalopathy, lactic acidosis and stroke-like episodes. *Mitochondrion* **2011**, *11*, 615–619.

Gordon, K.; Clouaire, T.; Bao, X.X.; Kemp, S.E.; Xenophontos, M.; de Las Heras, J.I.; Stancheva, I. Immortality, but not oncogenic transformation, of primary human cells leads to epigenetic reprogramming of DNA methylation and gene expression. *Nucleic Acids Res.* **2014**, *42*, 3529–3541.

Govatati, S.; Deenadayal, M.; Shivaji, S.; Bhanoori, M. Mitochondrial displacement loop alterations are associated with endometriosis. *Fertil. Steril.* **2013**, *99*, 1980-1986.e9.

Guan, J.-L.; Simon, A.K.; Prescott, M.; Menendez, J.A.; Liu, F.; Wang, F.; Wang, C.; Wolvetang, E.; Vazquez-Martin, A.; Zhang, J. Autophagy in stem cells. *Autophagy* **2013**, *9*, 830–849.

Gupta, G.P.; Massagué, J. Cancer metastasis: building a framework. *Cell* **2006**, *127*, 679–695.

Horváth, R.; Bender, A.; Abicht, A.; Holinski-Feder, E.; Czermin, B.; Trips, T.; Schneiderat, P.; Lochmüller, H.; Klopstock, T. Heteroplasmic mutation in the anticodon-stem of mitochondrial tRNA(Val) causing MNGIE-like gastrointestinal dysmotility and cachexia. *J. Neurol.* **2009**, *256*, 810–815.

Ince, T.A.; Richardson, A.L.; Bell, G.W.; Saitoh, M.; Godar, S.; Karnoub, A.E.; Iglehart, J.D.; Weinberg, R.A. Transformation of different human breast epithelial cell types leads to distinct tumor phenotypes. *Cancer Cell* **2007**, *12*, 160–170.

Joshi, A.; Kundu, M. Mitophagy in hematopoietic stem cells: the case for exploration. *Autophagy* **2013**, *9*, 1737–1749.

Kang, K.S.; Morita, I.; Cruz, A.; Jeon, Y.J.; Trosko, J.E.; Chang, C.C. Expression of estrogen receptors in a normal human breast epithelial cell type with luminal and stem cell characteristics and its neoplastically transformed cell lines. *Carcinogenesis* **1997**, *18*, 251–257.

Kang, K.S.; Sun, W.; Nomata, K.; Morita, I.; Cruz, A.; Liu, C.J.; Trosko, J.E.; Chang, C.C. Involvement of tyrosine phosphorylation of p185(c-erbB2/neu) in tumorigenicity induced by X-rays and the neu oncogene in human breast epithelial cells. *Mol. Carcinog.* **1998**, *21*, 225–233.

Kao, C.Y.; Nomata, K.; Oakley, C.S.; Welsch, C.W.; Chang, C.C. Two types of normal human breast epithelial cells derived from reduction mammoplasty: phenotypic characterization and response to SV40 transfection. *Carcinogenesis* **1995**, *16*, 531–538.

Kao, C.-Y.; Oakley, C.S.; Welsch, C.W.; Chang, C.-C. Growth requirements and neoplastic transformation of two types of normal human breast epithelial cells derived from reduction mammoplasty. *In Vitro Cellular & Developmental Biology - Animal* **1997**, *33*, 282–288.

Keller, P.J.; Arendt, L.M.; Skibinski, A.; Logvinenko, T.; Klebba, I.; Dong, S.; Smith, A.E.; Prat, A.; Perou, C.M.; Gilmore, H.; et al. Defining the cellular precursors to human breast cancer. *Proc. Natl. Acad. Sci. U.S.A.* **2012**, *109*, 2772–2777.

Kennedy, S.R.; Schmitt, M.W.; Fox, E.J.; Kohrn, B.F.; Salk, J.J.; Ahn, E.H.; Prindle, M.J.; Kuong, K.J.; Shen, J.-C.; Risques, R.-A.; et al. Detecting ultralow-frequency mutations by Duplex Sequencing. *Nat Protoc* **2014**, *9*, 2586–2606.

Levinger, L.; Oestreich, I.; Florentz, C.; Mörl, M. A pathogenesis-associated mutation in human mitochondrial tRNALeu(UUR) leads to reduced 3'-end processing and CCA addition. *J. Mol. Biol.* **2004**, *337*, 535–544.

Lou, D.I.; Hussmann, J.A.; McBee, R.M.; Acevedo, A.; Andino, R.; Press, W.H.; Sawyer, S.L. High-throughput DNA sequencing errors are reduced by orders of magnitude using circle sequencing. *Proc. Natl. Acad. Sci. U.S.A.* **2013**, *110*, 19872–19877.

McFarland, R.; Swalwell, H.; Blakely, E.L.; He, L.; Groen, E.J.; Turnbull, D.M.; Bushby, K.M.; Taylor, R.W. The m.5650G>A mitochondrial tRNAAla mutation is pathogenic and causes a phenotype of pure myopathy. *Neuromuscul. Disord.* **2008**, *18*, 63–67.

Meng, X.-L.; Meng, H.; Zhang, W.; Qin, Y.-H.; Zhao, N.-M. The role of mitochondrial tRNA variants in female breast cancer. *Mitochondrial DNA A DNA Mapp Seq Anal* **2016**, *27*, 3199–3201.

Park, J.-S.; Noh, D.-Y.; Kim, S.-H.; Kim, S.-H.; Kong, G.; Chang, C.-C.; Lee, Y.-S.; Trosko, J.E.; Kang, K.-S. Gene expression analysis in SV40-immortalized human breast luminal epithelial cells with stem cell characteristics using a cDNA microarray. *Int. J. Oncol.* **2004**, *24*, 1545–1558.

Pejaver, V.; Urresti, J.; Lugo-Martinez, J.; Pagel, K.A.; Lin, G.N.; Nam, H.-J.; Mort, M.; Cooper, D.N.; Sebat, J.; Iakoucheva, L.M.; et al. MutPred2: inferring the molecular and phenotypic impact of amino acid variants. *bioRxiv* **2017**.

Pickrell, A.M.; Huang, C.-H.; Kennedy, S.R.; Ordureau, A.; Sideris, D.P.; Hoekstra, J.G.; Harper, J.W.; Youle, R.J. Endogenous Parkin Preserves Dopaminergic Substantia Nigral Neurons following Mitochondrial DNA Mutagenic Stress. *Neuron* **2015**, *87*, 371–381.

Pipas, J.M. SV40: Cell transformation and tumorigenesis. *Virology* **2009**, *384*, 294–303.

Porcelli, A.M.; Ghelli, A.; Ceccarelli, C.; Lang, M.; Cenacchi, G.; Capristo, M.; Pennisi, L.F.; Morra, I.; Ciccarelli, E.; Melcarne, A.; et al. The genetic and metabolic signature of oncocytic transformation implicates HIF1alpha destabilization. *Hum. Mol. Genet.* **2010**, *19*, 1019–1032.

Salk, J.J.; Schmitt, M.W.; Loeb, L.A. Enhancing the accuracy of next-generation sequencing for detecting rare and subclonal mutations. *Nat. Rev. Genet.* **2018**, *19*, 269–285.

Santagata, S.; Thakkar, A.; Ergonul, A.; Wang, B.; Woo, T.; Hu, R.; Harrell, J.C.; McNamara, G.; Schwede, M.; Culhane, A.C.; et al. Taxonomy of breast cancer based on normal cell phenotype predicts outcome. *J. Clin. Invest.* **2014**, *124*, 859–870.

Saretzki, G.; Walter, T.; Atkinson, S.; Passos, J.F.; Bareth, B.; Keith, W.N.; Stewart, R.; Hoare, S.; Stojkovic, M.; Armstrong, L.; et al. Downregulation of multiple stress defense mechanisms during differentiation of human embryonic stem cells. *Stem Cells* **2008**, *26*, 455–464.

Schmitt, M.W.; Fox, E.J.; Prindle, M.J.; Reid-Bayliss, K.S.; True, L.D.; Radich, J.P.; Loeb, L.A. Sequencing small genomic targets with high efficiency and extreme accuracy. *Nat. Methods* **2015**, *12*, 423–425.

Schmitt, M.W.; Kennedy, S.R.; Salk, J.J.; Fox, E.J.; Hiatt, J.B.; Loeb, L.A. Detection of ultra-rare mutations by next-generation sequencing. *Proc. Natl. Acad. Sci. U.S.A.* **2012**, *109*, 14508–14513.

Sonney, S.; Leipzig, J.; Lott, M.T.; Zhang, S.; Procaccio, V.; Wallace, D.C.; Sondheimer, N. Predicting the pathogenicity of novel variants in mitochondrial tRNA with MitoTIP. *PLoS Comput. Biol.* **2017**, *13*, e1005867.

Strachan, T.; Read, A.P. *Human molecular genetics*; 2nd ed.; Wiley: New York, 1999; ISBN 978-0-471-33061-5.

Sun, W.; Kang, K.S.; Morita, I.; Trosko, J.E.; Chang, C.C. High susceptibility of a human breast epithelial cell type with stem cell characteristics to telomerase activation and immortalization. *Cancer Res.* **1999**, *59*, 6118–6123.

Tai, M.-H.; Chang, C.-C.; Kiupel, M.; Webster, J.D.; Olson, L.K.; Trosko, J.E. Oct4 expression in adult human stem cells: evidence in support of the stem cell theory of carcinogenesis. *Carcinogenesis* **2005**, *26*, 495–502.

Taylor, R.W.; Turnbull, D.M. Mitochondrial DNA mutations in human disease. *Nat. Rev. Genet.* **2005**, *6*, 389–402.

Vogelstein, B.; Kinzler, K.W. Cancer genes and the pathways they control. *Nat. Med.* **2004**, *10*, 789–799.

Wang, K.; Li, M.; Hakonarson, H. ANNOVAR: functional annotation of genetic variants from high-throughput sequencing data. *Nucleic Acids Res.* **2010**, *38*, e164.

Wang, K.-H.; Kao, A.-P.; Chang, C.-C.; Lee, J.-N.; Hou, M.-F.; Long, C.-Y.; Chen, H.-S.; Tsai, E.-M. Increasing CD44+/CD24(-) tumor stem cells, and upregulation of COX-2 and HDAC6, as major functions of HER2 in breast tumorigenesis. *Mol. Cancer* **2010**, *9*, 288.

Welm, B.; Behbod, F.; Goodell, M.A.; Rosen, J.M. Isolation and characterization of functional mammary gland stem cells. *Cell Prolif.* **2003**, *36 Suppl 1*, 17–32.

Fig 1

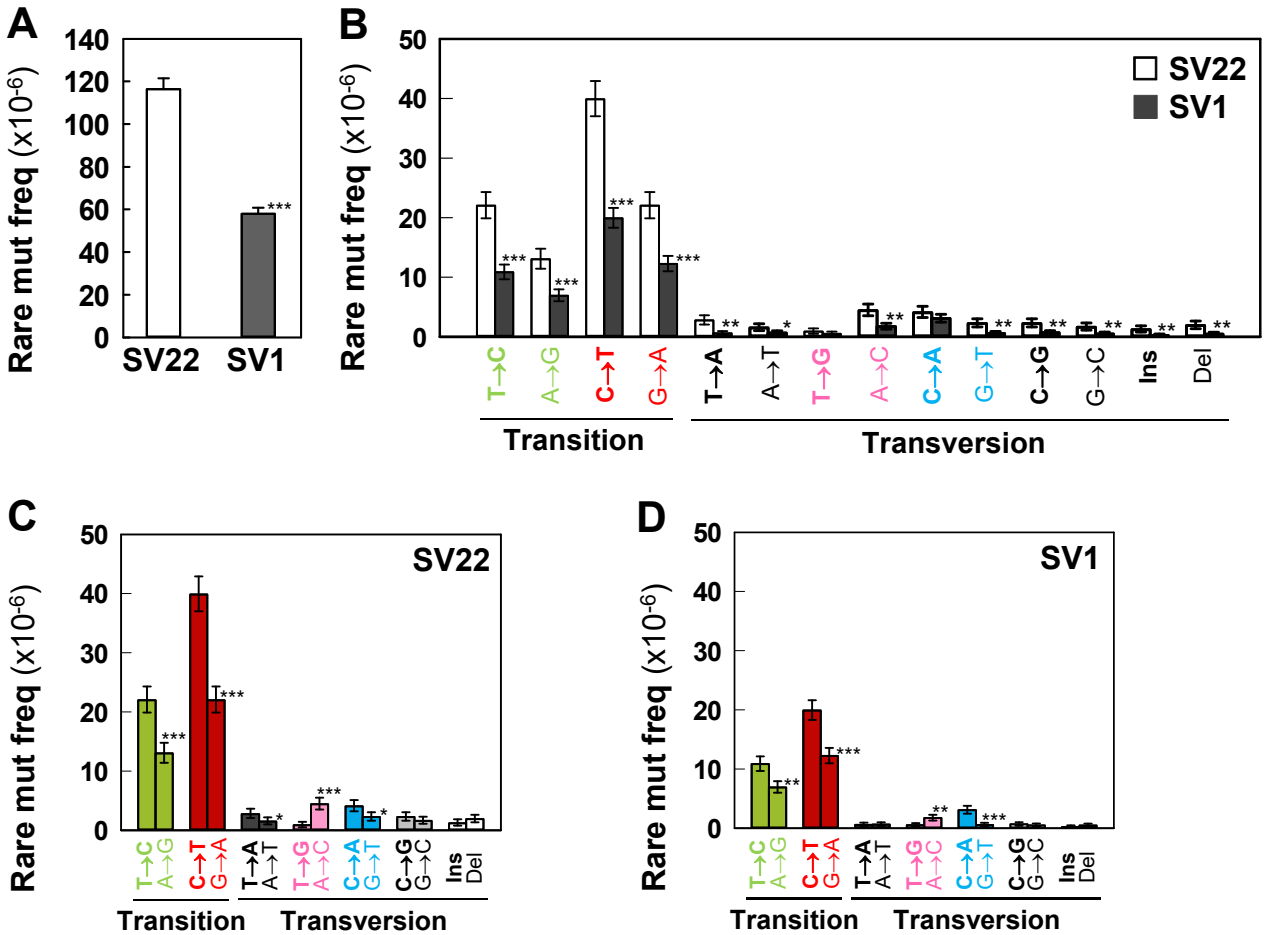
A
Rare mut freq (x10-6)
140
120
100
80
60
40
20
0
SV22
SV1
***
B
Rare mut freq (x10-6)
50
40
30
20
10
0
SV22
SV1
T→C
A→G
C→T
G→A
T→A
A→T
T→G
A→C
C→A
G→T
C→G
G→C
Ins
Del
Transition
Transversion
C
Rare mut freq (x10-6)
SV22
T→C
A→G
C→T
G→A
T→A
A→T
T→G
A→C
C→A
G→T
C→G
G→C
Ins
Del
Transition
Transversion
D
Rare mut freq (x10-6)
SV1
T→C
A→G
C→T
G→A
T→A
A→T
T→G
A→C
C→A
G→T
C→G
G→C
Ins
Del
Transition
Transversion

Fig 2

A

	C>A/ G>T	C>G/ G>C	C>T/ G>A	T>A/ A>T	T>C/ A>G	T>G/ A>C
SV22	6.0	3.8	49.4	4.2	31.3	5.3
SV1	8.5	2.6	53.2	2.9	29.2	3.6

B

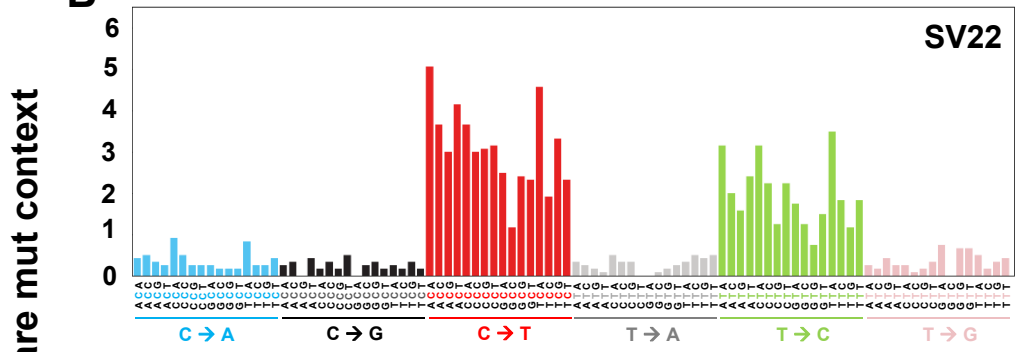

C

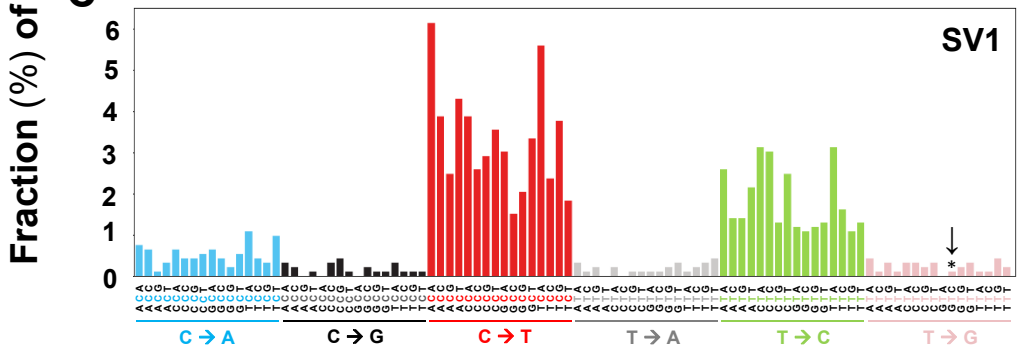

Fig 3

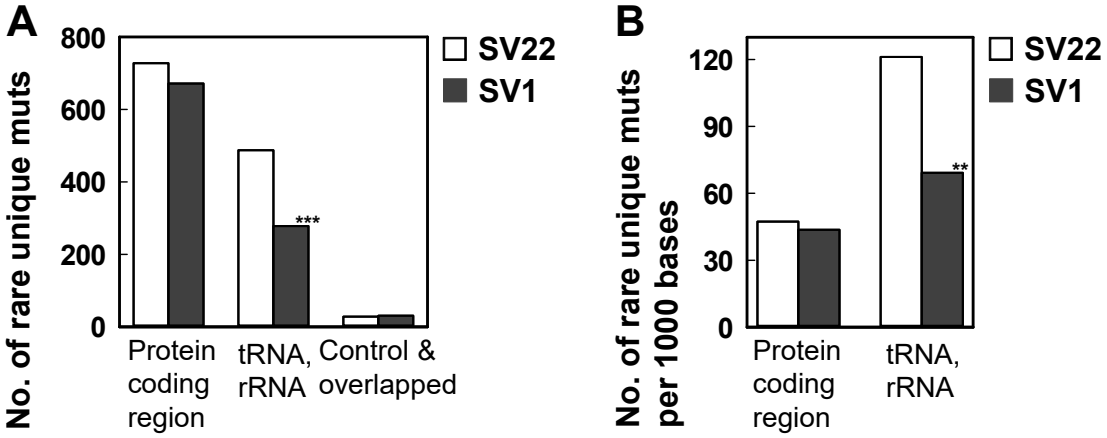
A
No. of rare unique muts
800
600
400
200
0
***
Protein coding region
tRNA, rRNA
Control & overlapped
SV22
SV1
B
No. of rare unique muts per 1000 bases
120
90
60
30
0
**
Protein coding region
tRNA, rRNA
SV22
SV1

Fig 4

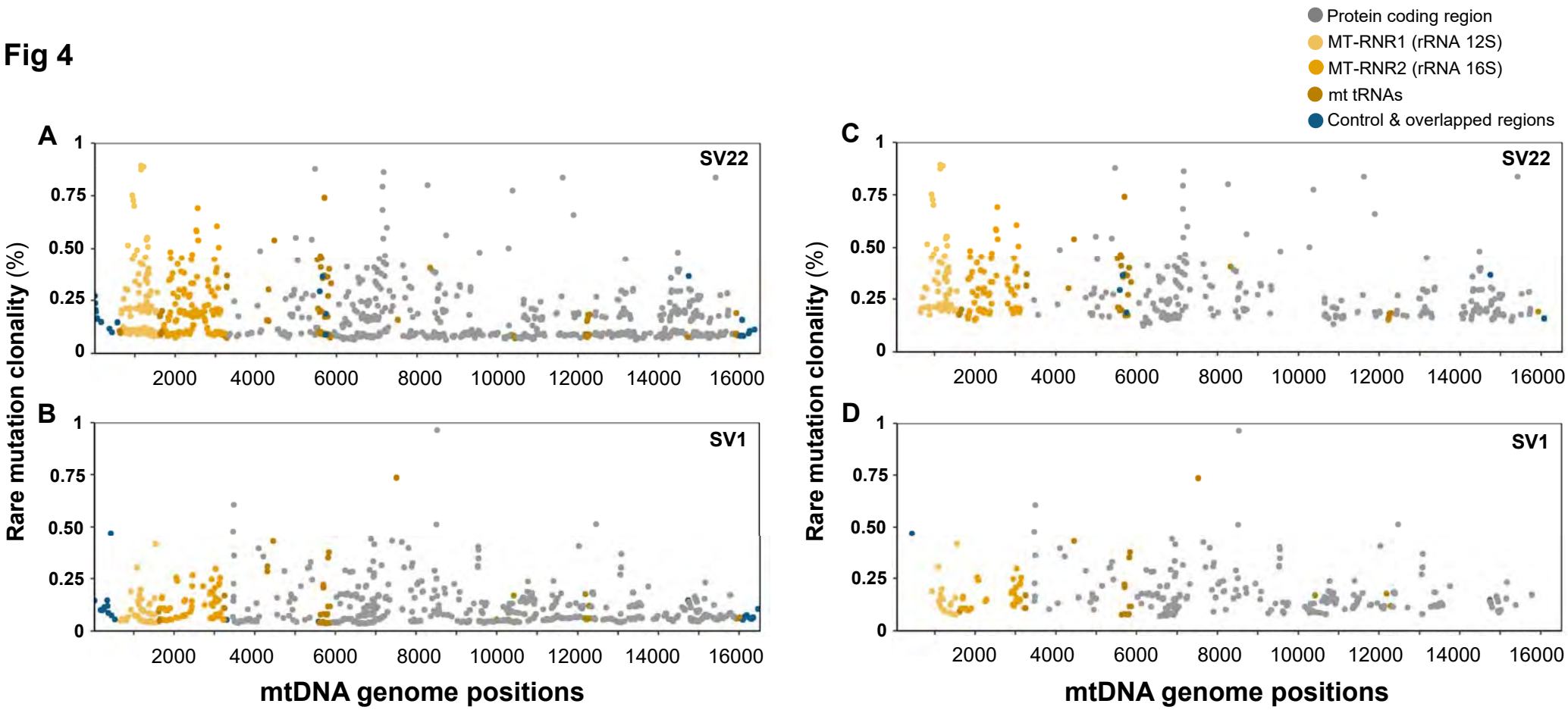
Protein coding region
MT-RNR1 (rRNA 12S)
MT-RNR2 (rRNA 16S)
mt tRNAs
Control & overlapped regions
A
B
C
D
SV22
SV1
SV22
SV1
Rare mutation clonality (%)
Rare mutation clonality (%)
0
0.25
0.50
0.75
1
2000
4000
6000
8000
10000
12000
14000
16000
mtDNA genome positions
mtDNA genome positions

Fig 5

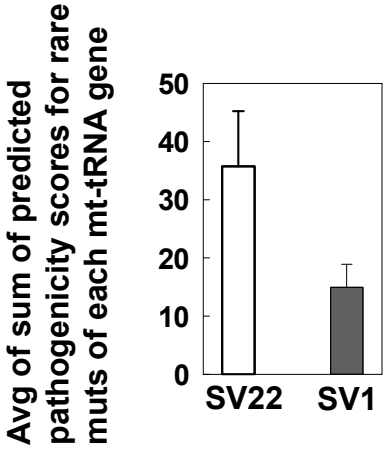
Avg of sum of predicted pathogenicity scores for rare muts of each mt-tRNA gene
50
40
30
20
10
0
SV22
SV1